However, under conditions of anomalous transmission, it is found that only those crystal imperfections lying quite close to the exit surface give well-defined images. It is to be noted that since imperfect regions destroy the conditions for the anomalously low absorption, they produce less blackening on the emulsion than the more perfect crystal regions surrounding them. This type of contrast is the reverse of that obtained with $\mu t \leqslant 1$, when imperfections make themselves manifest by their extra diffracting power.

Applications. Since the discovery in 1957 that individual dislocations could be imaged in X-ray diffraction topographs, activity with the X-ray topographic technique has increased. This particular application will be dealt with separately in the article on "Dislocation Studies by X-ray Diffraction Topography" (q.v.). However, informative topographs can be obtained even when dislocations cannot be individually resolved, and many other types of imperfection can be studied. Misorientations, growth stratifications, inclusions and precipitates have been studied in natural crystals such as diamond, quartz and calcite. For laboratory-grown crystals the Schulz method is very convenient for a quick check of crystal perfection; its applications to aluminum have been described by Kelly and Wei[17] and Doherty and Davis.[12] Transmission methods, using characteristic radiation, have been used to study precipitates in silicon, diffraction contrast due to variation of oxygen content in silicon,[30] and stacking faults in silicon.[18] Defects in whiskers and thin platelike crystals are also conveniently studied by transmission methods.[31, 32] The Berg-Barrett method has been used to study impurity substructures in zinc[16] and has found much application in studies of deformation structures in metals.[15, 24] More recently, transmission methods have been used to map magnetic domains[25] and to investigate the effects of radiation damage.

X-ray diffraction topography cannot compete with the resolution of the electron microscope. The best X-ray topographic resolution obtained in both reflection and transmission arrangements is about one micron, and several factors make it extremely difficult to better this figure. However, the ability to make repetitive, nondestructive examinations of large crystal specimens is a virtue of the X-ray techniques which frequently finds advantageous employment, as in the sample of applications listed above.

References

1. Barrett, C. S., *Trans. A.I.M.E.* **161,** 15 (1945)
2. Barth, H., and Hosemann, R., *Z. Naturforsch.* **13a,** 792 (1958)
3. Berg, W. F., *Wiss. Veröffentl. Siemens-Werken* **9,** 119 (1930)
4. Berg, W. F., *Naturwiss.* **19,** 391 (1931)
5. Bond, W. L., and Andrus, J., *Am. Mineralogist,* **37,** 622 (1952)
6. Bonse, U., "Direct Observation of Imperfections in Crystals," p. 431, eds. Newkirk and Wernick, New York, Interscience Publishers, Inc., 1962.
7. Bonse, U., and Kappler, E., *Z. Naturforsch.* **13a,** 348 (1958)
8. Borrmann, G., *Physik. Z.* **42,** 157 (1941)
9. Borrmann, G., *Z. Phys.* **127,** 297 (1950)
10. Cosslett, V. E., and Duncomb, P., *Nature* **177,** 1172 (1956)
11. Coyle, R. A., Marshall, A. M., Auld, J. H., and McKinnon, N. A., *Brit. J. Appl. Phys.* **8,** 79 (1957)
12. Doherty, P. E., and Davis, R. S., *Acta Metallurgica,* **7,** 118 (1959)
13. Gerold, V., and Meier, F., *Z. Phys.* **155,** 387 (1959)
14. Hamós, L. von, *Nature* **134,** 181 (1934)
15. Honeycombe, R. W. K., *J. Inst. Metals* **80,** 39 (1951)
16. Hulme, K. F., *Acta Metallurgica* **2,** 810 (1954)
17. Kelly, A., and Wei, C. T., *J. Metals* **7,** 1041 (1955)
18. Kohra, K., and Yoshimatsu, M., *J. Phys. Soc. Japan* **17,** 1041 (1962)
19. Lang, A. R., *Acta Cryst.* **10,** 839 (A) (1957)
20. Lang, A. R., *Acta Metallurgica* **5,** 358 (1957)
21. Lang, A. R., *Acta Cryst.* **12,** 249 (1959)
22. Merlini, A., and Guinier, A., *Bull. soc. franç. mineral. crist.* **80,** 147 (1957)
23. Newkirk, J. B., *Trans. A.I.M.E.* **215,** 483 (1959)
24. Nishiyama, N., and Yamamoto, M., *Mem. Inst. Sci. Ind. Research Osaka Univ.* **11,** 163 (1954)
25. Polcarová, M., and Lang, A. R., *Appl. Phys. Letters* **1,** 13 (1962)
26. Ramachandran, G. N., *Proc. Indian Acad. Sci.* **A.19,** 280 (1944)
27. Renninger, M., *Z. Naturforsch.* **16a,** 1110 (1961)
28. Renninger, M., *Physics Letters* **1,** 104 (1962)
29. Schulz, L. G., *Trans. A.I.M.E.* **200,** 1082 (1954)
30. Schwuttke, G. H., "Direct Observations of Imperfections in Crystals," p. 497, eds. Newkirk and Wernick, New York, Interscience Publishers, Inc., 1962.
31. Webb, W. W., *J. Appl. Phys.* **31,** 194 (1960)
32. Webb, W. W., "Direct Observations of Imperfections in Crystals," p. 29, eds. Newkirk and Wernick, New York, Interscience Publishers, Inc., 1962.
33. Wooster, N., and Wooster, W. A., *Nature* **155,** 786 (1945)

A. R. LANG

TOPOGRAPHY, X-RAY DIFFRACTION, IN DISLOCATION STUDIES

Basic Experiments. In 1957 it was discovered that individual dislocations could be observed by X-ray diffraction topographic methods. In fact, within a short space of time this observation was made independently in several laboratories, using different experimental arrangements. Quite a variety of X-ray topographic techniques had been developed by this date and a number of them had the necessary resolution and sensitivity to make single dislocations detectable in crystals of fairly low dislocation density. A summary of the principal techniques is given in the article on X-ray Diffraction Topography to which reference may be made for background information on the experimental methods referred to here.

A rough idea of why dislocations can be seen can be gained from the following considerations. Imagine a single dislocation line embedded in a

matrix of perfect crystal. If a path is followed that approaches close to the dislocation an increasing tilt and curvature of the lattice is encountered. The perfect regularity of lattice planes is destroyed and the region close to the dislocation is rendered relatively imperfect from the X-ray diffraction point of view, i.e., it partakes increasingly of the characteristics of a mosaic crystal, of which a given volume will diffract much more strongly than the same volume in the surrounding perfect crystal. Remembering that X-ray topographic methods are capable of great sensitivity both in lattice-tilt measurements and in studies of point-by-point variations in reflecting power it becomes understandable that the strain field around a single dislocation should make a recognizable image on the topograph. In fact, with proper choice of diffraction conditions, the diffraction images of individual dislocations show up with intense extra blackening over an image width of several microns.

The first X-ray topographic studies of individual dislocations were made by Lang,[12] Newkirk,[18] Bonse and Kappler[3] and Borrmann, Hartwig and Irmler.[4] Lang used the method of "section topographs"[11] with the image formed by diffracted X-rays transmitted through the specimen. Newkirk used a refinement of the Berg-Barrett technique[19] with reflection of X-rays from the specimen surface. A reflection specimen was also used by Bonse and Kappler, but with strict collimation of the incident beam by prior reflection at a monochromator crystal. Borrmann *et al.* employed very different diffraction conditions, for they observed the shadows formed by dislocations in the narrow bands of radiation transmitted by a thick crystal placed close to a source of divergent characteristic X-rays so as to produce a wide-angle diffraction pattern. These narrow bands of radiation are just those which satisfy the Bragg condition exactly and are transmitted through the crystal with anomalously low absorption, the Borrmann effect. The dislocations locally destroy the lattice perfection needed for the Borrmann effect to operate, and hence cause a locally increased absorption of X-rays with correspondingly reduced blackening on the film. The contrast produced is thus the reverse of that given by dislocations in Newkirk's topographs, and in Lang's when lightly absorbing crystals are used. The earliest experiments had to check that there was a one-to-one correspondence between the diffraction images and known dislocations in the specimen. With reflection specimens this was done by comparing the X-ray topographs with the pattern of dislocation etch pits on the specimen surface, and with the transmission specimens of silicon used in early "section topographs" comparison could be made with the infrared transmission pictures after "decorating" the dislocations with copper precipitates by the method of Dash.[5] The next experiments had to investigate the variation in diffraction contrast of dislocations as a function of angle between the Bragg reflecting plane and the Burgers vector of the dislocation. The rules of visibility were established by Lang and Newkirk who systematized the procedure for the identification of Burgers vectors by comparing topographs of a selected series of X-ray reflections. This is more conveniently done with specimens in the transmission that the reflection arrangement, and with the development of the "projection topograph" and its use in preparing stereopictures,[13] means became available for studying the configuration of dislocations within relatively thick crystals and determining the Burgers vector of particular dislocation segments in their interior. Methods for obtaining topographs of extended regions of thick crystals diffracting under conditions of anomalous transmission have been described by Barth and Hosemann[1] and by Gerold and Meier,[8] but they suffer from the disadvantage that only dislocations close to the exit surface of the crystal give sharp images (unless they happen to be lying in the plane of the incident and diffracted X-rays) and when the Borrmann effect is strong it is impossible to make satisfactory stereopairs of topographs for studying the dislocations in depth.

Some Features of Dislocation Diffraction Contrast. The theory of the diffraction contrast given by dislocations in X-ray topographs is still under development. It is generally more complicated than that required to account adequately for the forms of dislocation images observed in electron microscopy, and only a few basic aspects of the X-ray case will be presented here. For individual dislocations to be resolvable in X-ray topographs the crystal must be such that the dislocations are separated from each other by at least a few microns and the intervening lattice is relatively perfect. Under such conditions the major volume fraction of the crystal behaves as perfect from the X-ray diffraction standpoint. Hence the dynamical diffraction theory for perfect crystals must be used to describe the underlying diffraction behavior of the crystal, with the effects of local perturbations due to lattice distortions at dislocations being taken into account. A useful summary of the dynamical theory, including special reference to its applications in diffraction topography, has been given by Webb.[20] For fuller treatments the texts of Zachariasen,[21] James[9] and von Laue[10] can be consulted.

Fortunately, the rules for identification of Burgers vectors may be understood without recourse to complex theory. The degree of diffraction contrast will vary with the strength of the component of lattice distortion normal to the Bragg reflecting planes. The maximum value of contrast obtainable depends in a complicated way on the X-ray scattering and absorbing power of the specimen material, the thickness of the specimen and the X-ray wavelength, and is not readily calculable. However, the criterion of invisibility, that there should be no component of lattice distortion perpendicular to the Bragg planes, applies under all diffraction conditions. To see further what this implies in the identification of Burgers vectors it is necessary to consider the form of the lattice distortions around dislocations. Figure 1 shows in perspective a block of crystal, assumed for simplicity to be based on a simple cubic lattice. If the

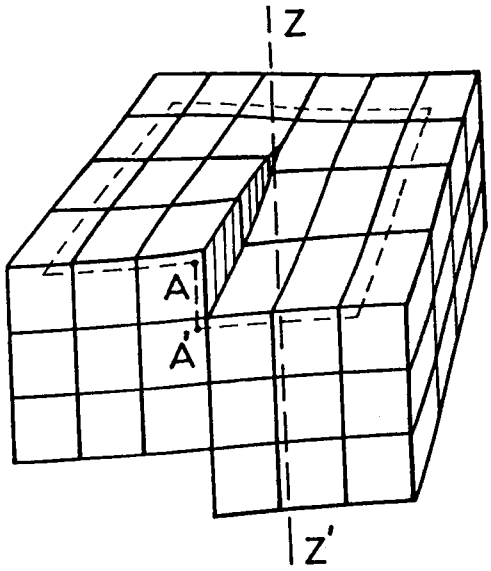

FIG. 1. Lattice distortion at a screw dislocation.

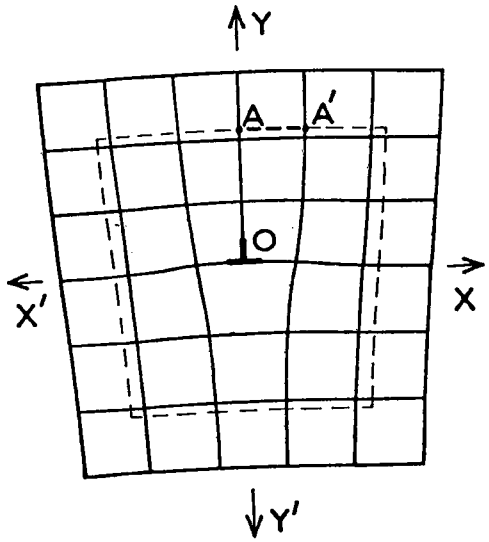

FIG. 2. Lattice distortion at an edge dislocation.

crystal is deformed by a pure screw dislocation which has its location along the vertical line ZZ' the block is distorted from its original parallelepiped form to take up the shape shown. The top surface, originally flat, now forms part of a helicoidal sheet. If a path is traversed over the top surface in such a way as to enclose the dislocation line then a vertical jump AA' must be included in order to make the path a closed circuit. This jump AA' is the Burgers vector and it lies parallel to the dislocation line ZZ' in the case of the pure screw dislocation. Of all the lattice planes that can be drawn in the crystal block, the maximum distortion is suffered by the top-surface plane which has the Burgers vector normal to it. It is to be especially noted that the vertical side planes of the block remain flat, and in fact any lattice plane in which ZZ' lies has no deformation component normal to its surface. For a general lattice plane a measure of the distortion normal to it is given by the scalar product, $\mathbf{b}.\mathbf{n}$, of the Burgers vector $\mathbf{b}$ and the unit vector $\mathbf{n}$ normal to the lattice plane. It follows that the rule for *invisibility* of a pure screw dislocation is simply that $\mathbf{b}.\mathbf{n} = 0$.

The lattice distortion at a pure edge dislocation is shown in Fig. 2. This depicts a single lattice plane. The edge dislocation passes perpendicularly through it at O and terminates the extra plane of atoms that has been inserted into the lattice and whose trace is OY. After the insertion of this plane an extra step AA' is required to close the circuit around O. Hence AA' is the Burgers vector $\mathbf{b}$, and it lies parallel to OX. Lattice planes perpendicular or inclined to the diagram and along whose normals AA' has a nonzero component are clearly distorted by the presence of the dislocation. However, even planes inclined to the diagram which intersect it parallel to XX' and hence have no component of $\mathbf{b}$ normal to them, suffer some distortion due to the dislocation. Thus, in the edge dislocation case, the condition $\mathbf{b}.\mathbf{n} = 0$ is not a sufficient criterion for invisibility. There is in fact only one plane in whose Bragg reflections the dislocation is quite invisible and that is the plane parallel to the diagram, i.e., perpendicular to the line of the pure edge dislocation. All distortions of the lattice lie in this plane and have no component normal to it.

In the more general case of a mixed dislocation, that is, one which can be formed by a combination of edge and screw components, the angle between the Burgers vector $\mathbf{b}$ and the vector $\mathbf{l}$ parallel to the dislocation line will take some value between 0° and 90°. The criterion of least visibility for the general case is that $\mathbf{b}.\mathbf{n} = 0$ and that, in addition, $\mathbf{b} \times \mathbf{n}.\mathbf{l} = 0$, the latter condition being contributed by the edge component. Thus, in words, not only must the Burgers vector and reflecting-plane normal be perpendicular to each other, but the Burgers vector, reflecting-plane normal and dislocation line must also be coplanar. The procedure for identification of Burgers vectors is straightforward. In principle, if any dislocation is found to be invisible in two reflections its Burgers vector must lie parallel to the line of intersection of the two reflecting planes. In practice, additional evidence is obtained by noting relative visibility in a number of X-ray reflections. It helps if diffraction conditions can be chosen to maximize the contribution of the factor $\mathbf{b}.\mathbf{n}$ to dislocation visibility. An idea which experimental situations best realize these conditions may be gained from the following brief consideration of the nature of dislocation images. Very roughly, one may divide the region around a dislocation into two concentric zones. The inner one contains lattice distortions which are so great that the crystal behaves as a mosaic, with large phase differences, rapidly varying functions of position, introduced between X-rays scattered from different parts of it. In the outer zone the distortion is more gentle, so that coherence between scattered waves is maintained but still some phase differences are introduced that are absent in the surrounding perfect matrix. The more smoothly varying phase differences cause a bending of the paths of the beams comprising the interacting primary and diffracted X-rays at very near to the Bragg angle. Next consider a

ray paths under the geometry of "section topographs" and "projection topographs," remembering that the image formed in a projection topograph can be regarded as the superimposition of many section topograph images. Suppose the crystal specimen has the form of a parallel-sided plate with the reflecting planes normal to it. Figure 3 shows three situations each with a narrow beam of characteristic radiation incident at O on the X-ray entrance surface of the specimen and radiation leaving the specimen over the region AB on the exit surface. The directions of incident and diffracted rays are parallel to OA and OB respectively, hence the angle $AOB = 2\theta$. The incident beam has typically a divergence of 1′ or 2′ of arc in the plane of the diagram. This angular range fully covers the range of reflection of a perfect crystal which is only a few seconds of arc. In an undistorted crystal, Fig. 3(a), X-ray energy flows down through the triangle, OAB, forming a fan of rays as shown. The center ray, parallel to the Bragg planes, is the path of energy-flow when the Bragg condition is exactly satisfied. When the angle of incidence is on the wings of the reflection curve the rays take paths approaching the directions OA and OB. At the exit surface the beams within the crystal split up as shown into primary rays travelling parallel to OA and diffracted rays travelling parallel to OB. The latter are received on the film and form the "section topograph." Suppose, as in Fig. 3(b), a dislocation line normal to the plane of the diagram lies within the triangle OAB. The two zones around the dislocation, the outer one of coherent scattering and the inner one of incoherent scattering, are shown on a greatly exaggerated scale. In actuality the diameter of the outer zone would be not greater than about 50 microns whereas the specimen thickness would be of the order of 1 mm. Refraction of rays in the outer zone causes a redistribution of energy over AB, whereas the inner zone acts somewhat as a scattering object in the ray paths, diverting some rays into the OA and OB directions. A different situation arises in Fig. 3(c) where the incident beam cuts through the center of the dislocation. The "mosaic" inner zone of the dislocation can reflect an appreciable fraction of the energy within the angular range of the incident beam, and it produces an intense diffracted beam which overshadows the other rays travelling in the triangle OAB. This intenser, sharper image is termed the "direct image," and the diffuse, weaker image arising from the outer zone is called the "dynamical

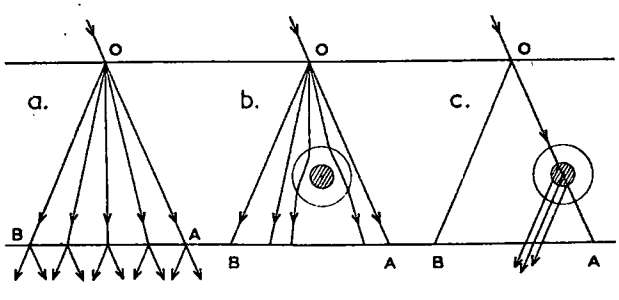

FIG. 3. Geometry of dislocation image formation.

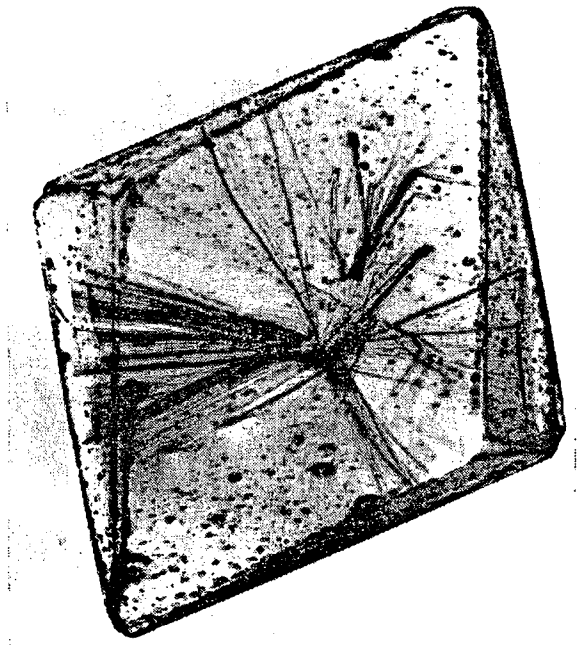

FIG. 4. Projection topograph showing dislocations in a diamond.

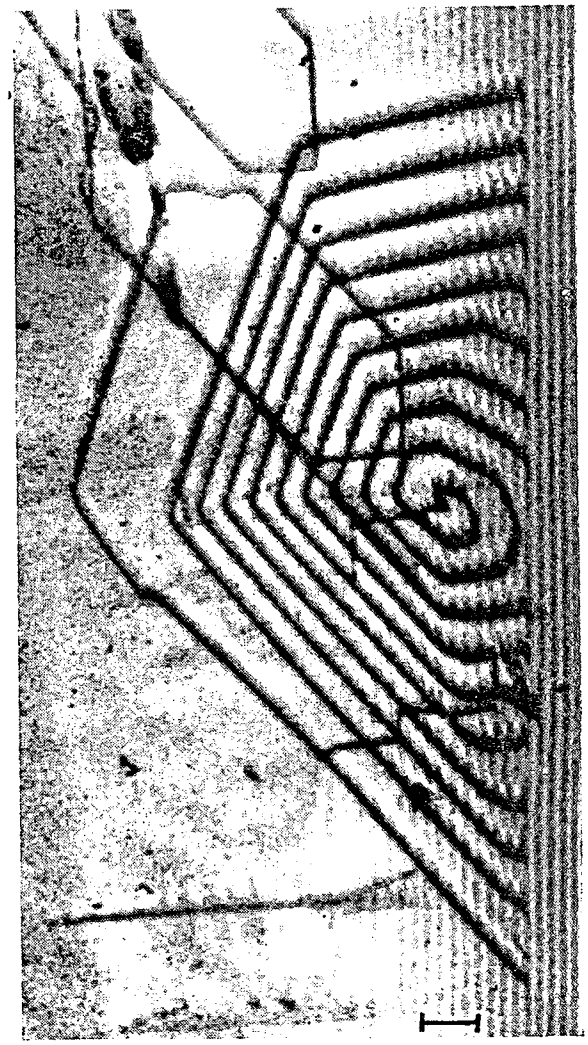

FIG. 5. Projection topograph of dislocation source in silicon. Scale mark 100 μ.